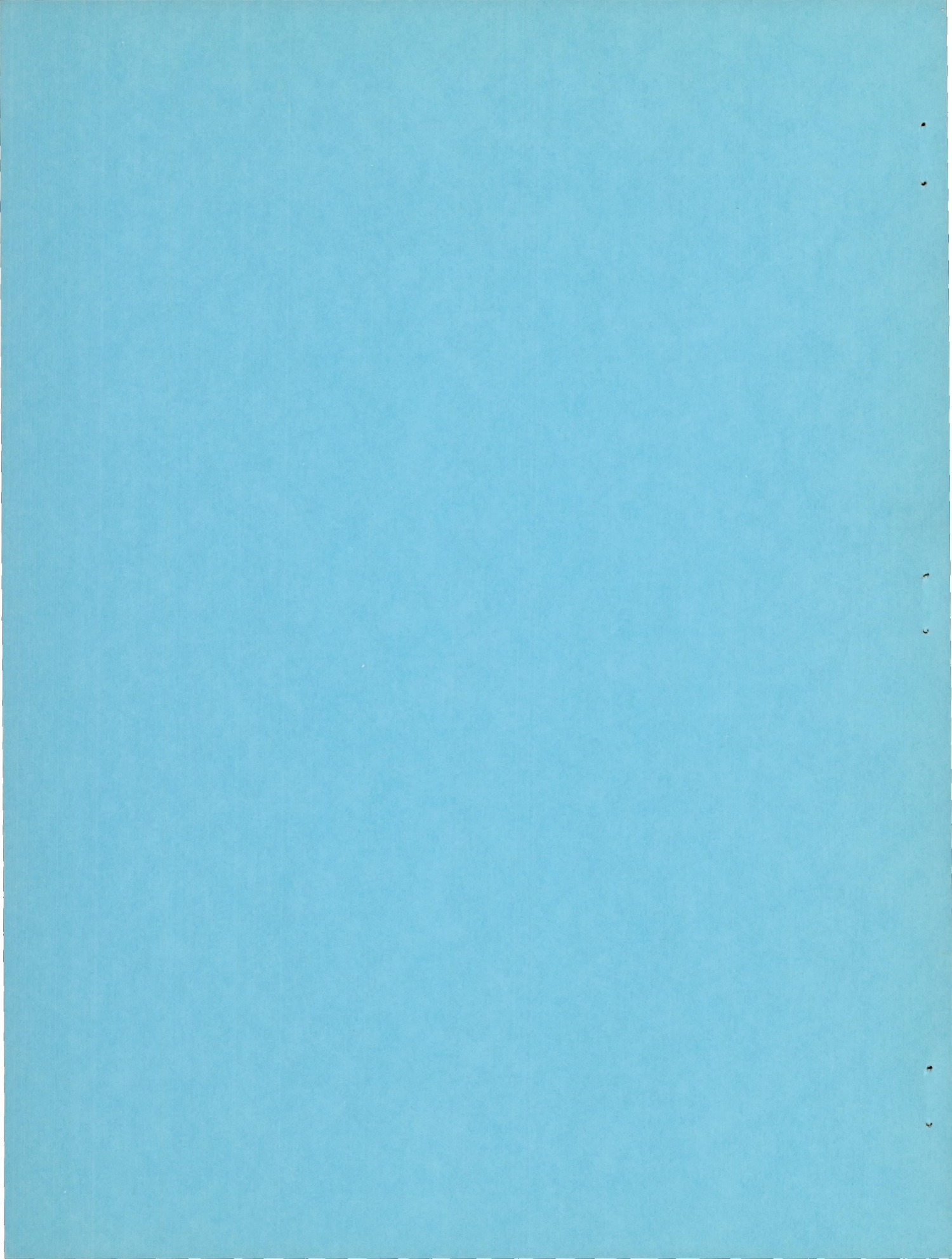# NACA

RESEARCH MEMORANDUM

FUSELAGE PRESSURES MEASURED ON THE BELL X-1 RESEARCH

AIRPLANE IN TRANSONIC FLIGHT

By Ronald J. Knapp, Gareth H. Jordan,
and Wallace E. Johnson

Langley Aeronautical Laboratory
Langley Field, Va.

NATIONAL ADVISORY COMMITTEE
FOR AERONAUTICS
WASHINGTON

November 6, 1953
Declassified November 30, 1956

NATIONAL ADVISORY COMMITTEE FOR AERONAUTICS

RESEARCH MEMORANDUM

FUSELAGE PRESSURES MEASURED ON THE BELL X-1 RESEARCH

AIRPLANE IN TRANSONIC FLIGHT

By Ronald J. Knapp, Gareth H. Jordan,
and Wallace E. Johnson

SUMMARY

Pressure-distribution measurements have been made on the fuselage of the Bell X-1 research airplane. Data are presented for angles of attack from 2° to 8° during pull-ups at Mach numbers of about 0.78, 0.85, 0.88, and 1.02.

The results of the investigation indicated that a large portion of the load carried by the fuselage was in the vicinity of the wing and may be attributed to wing-to-fuselage carryover. The presence of the wing from the 41 to 60 percent fuselage stations influenced the fuselage pressures from about 30 to 65 percent fuselage length at Mach numbers of approximately 0.78, 0.85, and 0.88, and from about 35 to 80 percent fuselage length at a Mach number of approximately 1.02.

The fuselage contributed about 20 percent of the total airplane normal-force coefficient. The center of pressure of the fuselage load throughout the tests was located from 41 to 51 percent fuselage length, which corresponds to the forward half of the wing root-chord location.

INTRODUCTION

The NACA High-Speed Flight Research Station at Edwards Air Force Base, Calif., has conducted a series of flight tests in the subsonic and transonic speed range on the Bell X-1 research airplane for the measurement of wing and fuselage pressure distributions. An analysis of the wing-section pressure distributions obtained at various spanwise stations on this airplane is given in reference 1. The spanwise wing-load distributions including some wing-to-fuselage carryover data are presented in reference 2. An analysis of the pressures measured on the base and rear portion of the fuselage at transonic speeds, including jet effects of the rocket engine, is presented in reference 3.

The purpose of this paper is to present an analysis of the pressure-distribution data obtained on the fuselage of this airplane along six longitudinal rows. The data were obtained during pull-ups to high lift (power-off condition) at Mach numbers of approximately 0.78, 0.85, 0.88, and 1.02 at altitudes from about 22,000 feet at the lower Mach numbers to 48,000 feet at the higher Mach numbers.

SYMBOLS

C_{m_F} fuselage pitching-moment coefficient about fuselage zero station, $\dfrac{-L}{\pi R} \displaystyle\int_0^1 \dfrac{x}{L} \dfrac{r}{R} c_n \, d\!\left(\dfrac{x}{L}\right)$

C_{N_A} airplane normal-force coefficient based on wing area, nW/qS

C_{N_F} fuselage normal-force coefficient based on maximum fuselage cross-sectional area, $\dfrac{L}{\pi R} \displaystyle\int_0^1 \dfrac{r}{R} c_n \, d\!\left(\dfrac{x}{L}\right)$

c_n fuselage station normal-force coefficient, $2 \displaystyle\int_0^1 P_R \, d\!\left(\dfrac{y}{r}\right)$

L fuselage length, 31 ft

M free-stream Mach number

n normal-load factor

P pressure coefficient, $\dfrac{p - p_o}{q}$

P_R resultant pressure coefficient, $P_L - P_U$

p local static pressure, lb/sq ft

p_o free-stream static pressure, lb/sq ft

q free-stream dynamic pressure, lb/sq ft

R maximum fuselage radius, 2.29 ft

r local fuselage radius, ft

S   wing area, including area projected through fuselage,
             130 sq ft

W   airplane weight, lb

x   longitudinal fuselage coordinate, ft

y   lateral fuselage coordinate, r cos θ, ft

α   fuselage angle of attack, deg

θ   angular fuselage coordinate (fig. 3), deg

Subscripts:

L   lower half of fuselage

U   upper half of fuselage

cr   critical (value for which the local flow becomes sonic)

max   maximum

DESCRIPTION OF AIRPLANE

The Bell X-1 rocket-propelled research airplane used in these tests
and the general overall dimensions are shown in the photograph and
three-view drawing presented as figures 1 and 2, respectively.

The airplane fuselage is a sharp-nosed modified body of revolution
having a fineness ratio of 6.8, with the maximum diameter located at
about 39 percent of the fuselage length. A line through the centers of
the various fuselage sections sweeps upward gradually from the 79-percent
station to the fuselage base, where it is 5.5 inches above the center
line of the airplane. The circular cross section of the fuselage is
modified rearward of the 79-percent station, tapering gradually to a
cloverleaf - shaped section at the fuselage base to accommodate the
four-nozzled rocket engine. In order to accommodate the control rods,
plumbing, and wiring, dorsal and ventral fairings were added to the
fuselage as shown in figures 1 to 3. For purpose of integration of pres-
sures over the body, the fuselage is treated as a simple body of revolu-
tion, the coordinates of which are given in figure 3.

The airplane had a 10-percent-thick wing (modified NACA 65-110 air-
foil section) with an aspect ratio of 6, taper ratio of 0.5, washout of
1°, and was unswept at the 40-percent-chord line. The wing was mounted

approximately on the center line of the fuselage with an incidence at
the root of 2.5° with respect to the center line. The wing leading and
trailing edges at the wing-panel root were located at about 41 and
60 percent of the fuselage length, respectively.

INSTRUMENTATION AND DATA REDUCTION

Standard NACA instrumentation was used to measure all fuselage sur-
face pressures (using two NACA 60-cell recording flight manometers),
normal acceleration, and angles of attack and sideslip. Indicated free-
stream static and dynamic pressures were measured with an NACA high-speed
pitot-static tube. All records were synchronized by a common timer.
Mach number and free-stream static pressure were obtained from the indi-
cated free-stream static and dynamic pressures by the radar tracking
method of reference 4. The total pressure tube was of the cylindrical-
cavity type described as tube A-6 in reference 5. This tube was used
because of its insensitiveness to angle of attack. The static vents
were located 0.6 maximum fuselage diameter ahead of the fuselage nose.
All surface pressures were measured relative to the pressure in the
instrument compartment. The instrument compartment pressure was meas-
ured relative to the indicated free-stream static pressure, which was
corrected to the true free-stream static pressure as described.

Fuselage surface pressures were obtained over the left side of the
fuselage from 1/8-inch-diameter flush-type orifices installed in the
surface. The locations of the orifices are given in figure 3. The
orifices were connected to the instrument compartment by 5/32-inch
inside-diameter aluminum tubing. The length of aluminum tubing varied
from about 2 feet at the center section to about 17 feet at the extreme
forward and rearward stations. Approximately 3 feet of 3/16-inch inside-
diameter rubber tubing was used to connect each aluminum tube to the
manometer cell. The effects of lag in the measurement of surface pres-
sures have been neglected inasmuch as these effects have been found to
be insignificant at the rates at which pressures were changing during
these tests.

The fuselage-section pressure-distribution plots were mechanically
integrated around the fuselage to obtain station normal-force coefficients,
which were used to construct longitudinal load-distribution plots. These
plots were mechanically integrated to obtain fuselage normal-force coef-
ficients C_{N_F} and pitching-moment coefficients C_{m_F} from which center-
of-pressure locations were obtained. The data were worked up for small
increments of C_{N_A}. Interpolations between these values have been deemed
allowable and have been used to obtain the data at angles of attack of 2°,
4°, 6°, and 8°.

TESTS

The data presented were obtained during pull-ups to high lift
(power-off condition) at Mach numbers of about 0.78, 0.85, 0.88, and
1.02. Each of the pull-ups was made at a nearly constant Mach number
except the pull-up at $M \approx 1.02$, which varied from $M = 1.11$ at low
lift to $M = 0.96$ at high lift. The altitude varied from about
22,000 feet at the lower Mach numbers to 48,000 feet at the higher Mach
numbers. Sideslip angles were small ($\pm 1°$) for all data presented.

ACCURACY

Estimates based on the accuracy of the recording instruments and
methods of calibration indicate that the measured quantities are accu-
rate to within the following limits:

M . . . . ± 0.01
P . . . . ± 0.03
α, deg . . . . ± 0.5

Estimates, based on the accuracies of the measured quantities,
integrative methods, and the coverage of the test data indicate that
the integrated quantities are accurate to within the following limits:

c_n . . . . ± 0.05
C_{N_F} . . . . ± 0.05
Center of pressure, percent . . . . ± 2

RESULTS AND DISCUSSION

Pressure Distribution

The pressure distributions obtained along the fuselage of the
Bell X-1 research airplane are shown in figure 4 for angles of attack
from $2°$ to $8°$. For an indication of the approximate airplane normal-
force coefficient corresponding to the angles of attack, figure 5 is
presented.

At an angle of attack of $2°$ (fig. 4(a)) the pressure distributions
are similar in shape and magnitude throughout the Mach number range
tested and similar for all fuselage rows (upper and lower) except in
the region influenced by the wing pressures. An exception to this

similarity of the pressure distributions along all orifice rows occurred at the forward end of the dorsal and ventral fairings (about 17.5 percent fuselage length) where the surface discontinuity caused the increased pressures seen on rows A and F.

The effect of varying the angle of attack from 2° to 8° (fig. 4(a) to 4(d)) was small forward of the region of wing influence and negligible rearward of this region. The pressure distributions show that forward of the region of wing influence there was a pressure variation with radial position, which increased gradually around the fuselage from the top (row A) to the bottom (row F). This effect increased with an increase in angle of attack from 2° to 8°.

The presence of the wing from 41 to 60 percent fuselage length influenced the fuselage pressures from about 30 to 65 percent fuselage length at $M \approx 0.78$, 0.85, and 0.88, and from about 35 to 80 percent fuselage length at the low supersonic Mach numbers tested. The pressure distributions along fuselage rows D and C between the leading and trailing edges of the extended wing, in general, show a similarity to those presented in reference 1 for the wing-root station throughout the Mach number and angle-of-attack range of these tests. Near the leading edge, however, the lower-surface stagnation and the upper-surface expansion were somewhat diminished on fuselage rows D and C. The fuselage rows nearer the airplane center line had pressure distributions with less similarity than those at rows D and C. A comparison indicating similar results are shown in reference 2 which used differential-pressure distributions along the wing-panel root station and those obtained along the fuselage rows in the area between the extended leading and trailing edges of the wing. The differential pressures, in general, became smaller as the center line of the airplane was approached.

For angles of attack from 2° to 8° (fig. 4) the pressure recovery that is apparent forward of the wing leading-edge position on rows D and C may be attributed to the positive pressure field associated with the wing leading-edge stagnation point. At all Mach numbers of the tests, the expansion along these rows, following the positive pressure region near the wing leading edge, may be accounted for by a pressure carryover from the expanded flow regions on the upper or lower surfaces of the wing.

A rapid pressure recovery is seen to occur on row C between 45 and 55 percent fuselage length at Mach numbers of about 0.78, 0.85, and 0.88 at angles of attack from 2° to 8° (fig. 4). The locations of these pressure-recovery regions were found in the comparison of reference 2 to be about the same as those on the wing-panel root station (due to the upper-wing-surface shock); this effect indicates a carryover of the wing shock to the fuselage in this region. For the pull-up at $M \approx 1.02$, the wing shock is located near the trailing edge throughout the lift

range, which accounts for the pressure recovery of row C being located near the wing trailing-edge location (fig. 4). As the center line of the airplane was approached, the pressure recovery became less steep and the shock location consequently less well-defined.

Normal Load

The longitudinal load distributions as obtained from the pressure distributions are shown in figure 6. It may be seen that, just as in the case of the pressure distributions, the loading did not vary appreciably with Mach number except in the region of wing influence. Also, only a small angle-of-attack effect may be seen on the loading in the regions not influenced by the wing. In these regions the loading parameter was small at all conditions of the tests.

Within the region where the fuselage pressure distributions were influenced by the wing there was a greatly increased loading, and there were significant Mach number and angle-of-attack effects on this loading. For a given angle of attack the peak value of loading parameter was largest at $M \approx 0.78$ and became successively smaller with an increase in Mach number. The peak became broader with an increase in Mach number, which partially compensated for this lower peak loading in contributing to the total load. Figure 6 shows an increased loading in this region of wing influence with an increase in angle of attack from 2° to 8° at all Mach numbers. It may be seen in these loadings that the influence of the wing accounts for a large portion of the fuselage load.

Figure 7 shows the approximate contribution of the fuselage load to the total airplane load $\left(C_{N_A} \approx 0.30 \text{ to } 0.70\right)$, along with the contribution of the wing panels (from ref. 2), and of the wing-fuselage combination. The fuselage is seen to carry close to 20 percent of the total airplane load throughout the Mach number range of the tests. The small deviation that occurred at Mach numbers from about 0.78 to 0.96 is believed to be associated with the change in angle of attack necessary to maintain a given C_{N_A} throughout the Mach number range. Tail loads were not measured on this airplane; however, it is expected that they would account for the deviation of the "wing and fuselage" curve from the 100-percent C_{N_A} line.

The variation of fuselage normal-force coefficient C_{N_F} with angle of attack (fig. 8) shows that for Mach numbers of 0.78 to 0.88, the lift curves were essentially linear to values of C_{N_F} of around 1.0. It is indicated that at Mach numbers of 0.96 and above the lift curves are linear to a higher angle of attack. There was no appreciable change in

lift-curve slope below $C_{N_F} \approx 1.0$ throughout the Mach number range tested. The high-speed pull-up with $M \approx 1.02$, because of a large change in Mach number, has been shown in this figure as two maneuvers at Mach numbers of approximately 1.05 and 0.96.

The approximate longitudinal fuselage center-of-pressure location is shown in figure 9. At a Mach number of approximately 0.78 a forward shift from 51 to 42 percent fuselage length occurred with an increase of C_{N_F} from approximately 0.4 to 1.1. At a Mach number of about 0.85, a similar center-of-pressure shift occurred; however, the low-lift center of pressure may be seen to be slightly rearward of that at $M \approx 0.78$. For $M \approx 0.88$, the center of pressure had only a small change throughout the lift range tested, shifting rearward from about 41 to 43 percent as C_{N_F} varied from about 0.7 to beyond 1.1. Similarly, there was only a small change in center of pressure during the pull-up in which the Mach number averaged 1.02 (shown as two parts at $M \approx 0.96$ and $M \approx 1.05$), where a variation from about 47 to 43 percent of fuselage length occurred in the C_{N_F} range from about 0.5 to 1.9. As may be seen from figure 6, these trends result from the fact that at the lower Mach numbers the loading in the region of wing influence and the loading on the forward part of the fuselage, relative to that over the rear part, each tend to move the center of pressure forward with increasing angle of attack, whereas at the higher Mach numbers they tend to cancel and, therefore, reduce the center-of-pressure movement.

CONCLUSIONS

Results of pressure-distribution measurements on the fuselage of the Bell X-1 research airplane during pull-ups at angles of attack from $2°$ to $8°$ and Mach numbers of about 0.78, 0.85, 0.88, and 1.02 indicate the following conclusions:

1. A large portion of the load carried by the fuselage was in the vicinity of the wing and may be attributed to wing-to-fuselage carryover.

2. The presence of the wing from the 41 to 60 percent fuselage stations influenced the fuselage pressures from about 30 to 65 percent fuselage length at Mach numbers of 0.78, 0.85, and 0.88, and from about 35 to 80 percent fuselage length at a Mach number of 1.02.

3. The fuselage contributed about 20 percent of the total airplane normal-force coefficient.

4. At Mach numbers of about 0.78 and 0.85, there was a definite forward center-of-pressure movement with an increase in fuselage normal-force coefficient. At the higher Mach numbers of the tests, the center-of-pressure movement with increasing load was small. Throughout these tests the center of pressure was located between about 41 and 51 percent fuselage length, which corresponds to the forward half of the wing root-chord location.

Langley Aeronautical Laboratory,
    National Advisory Committee for Aeronautics,
        Langley Field, Va., August 26, 1953.

REFERENCES

1. Knapp, Ronald J., and Jordan, Gareth H.: Flight-Determined Pressure Distributions Over the Wing of the Bell X-1 Research Airplane (10-Percent-Thick Wing) at Subsonic and Transonic Speeds. NACA RM L53D20, 1953.

2. Knapp, Ronald J., and Jordan, Gareth H.: Wing Loads on the Bell X-1 Research Airplane (10-Percent-Thick Wing) as Determined by Pressure-Distribution Measurements in Flight at Subsonic and Transonic Speeds. NACA RM L53G14, 1953.

3. Knapp, Ronald J., and Johnson, Wallace E.: Flight Measurements of Pressures on Base and Rear Part of Fuselage of the Bell X-1 Research Airplane at Transonic Speeds, Including Power Effects. NACA RM L52L01, 1953.

4. Zalovcik, John A.: A Radar Method of Calibrating Airspeed Installations on Airplanes in Maneuvers at High Altitudes and at Transonic and Supersonic Speeds. NACA Rep. 985, 1950. (Supersedes NACA TN 1979.)

5. Gracey, William, Coletti, Donald E., and Russell, Walter R.: Wind-Tunnel Investigation of a Number of Total-Pressure Tubes at High Angles of Attack. Supersonic Speeds. NACA TN 2261, 1951.
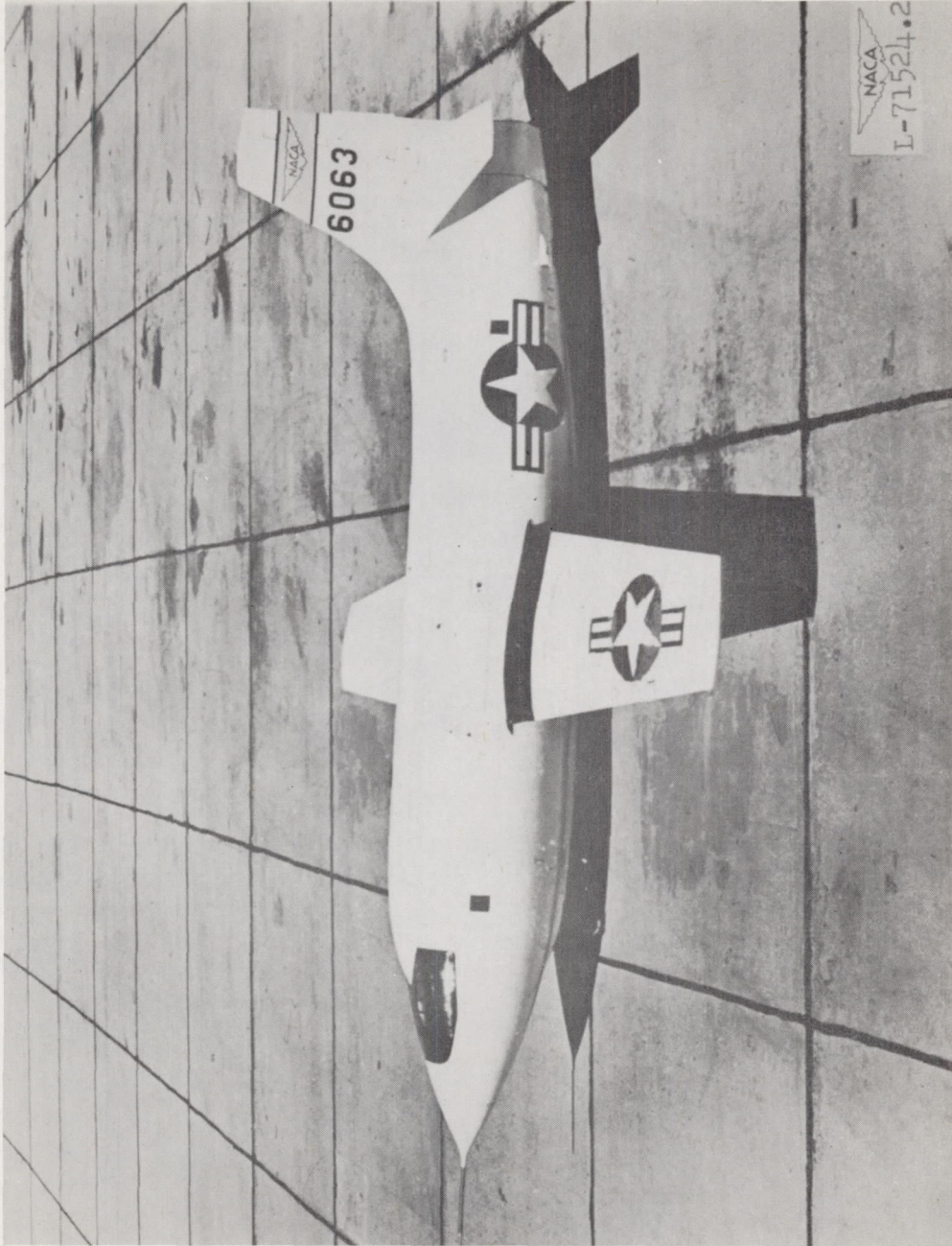
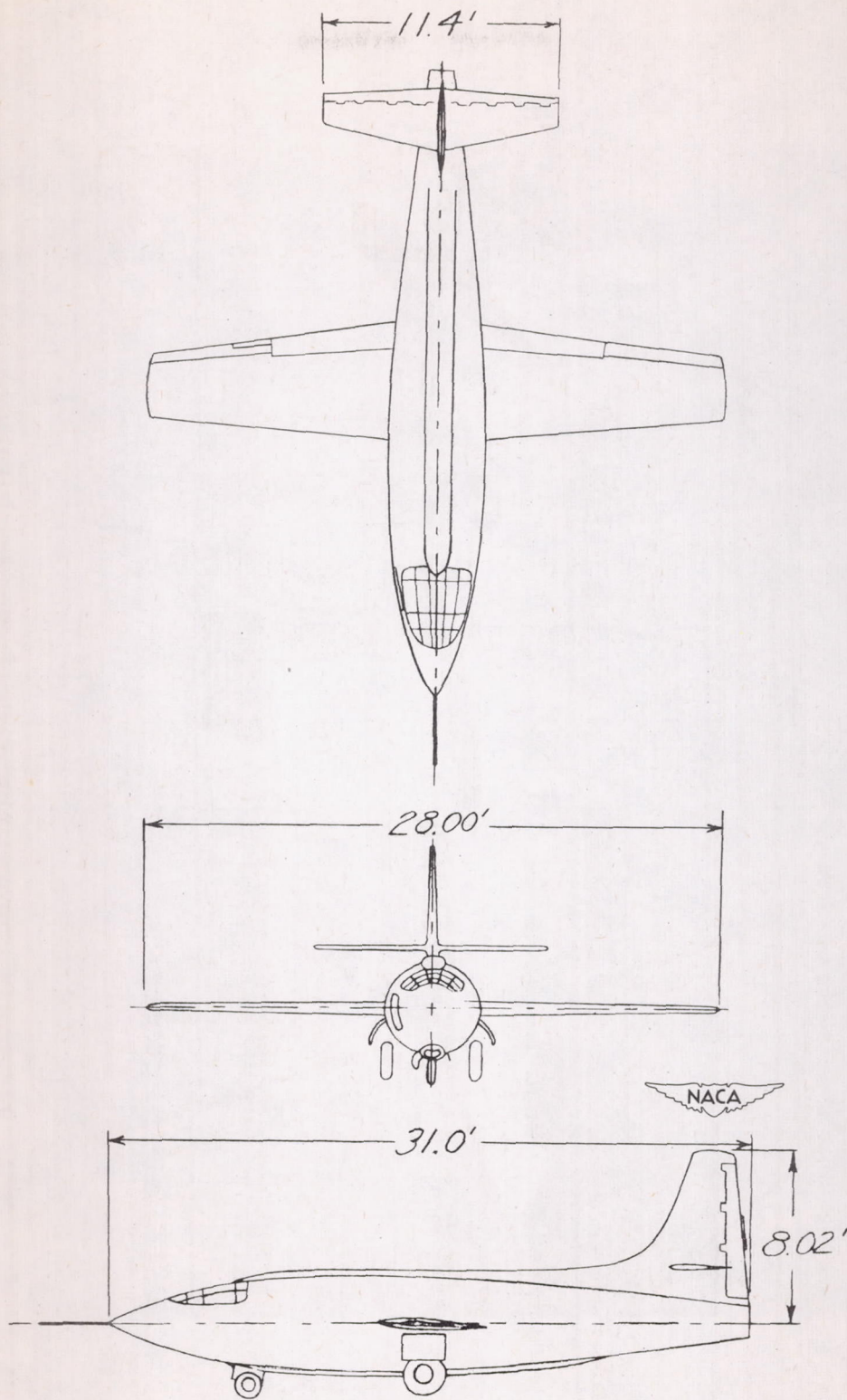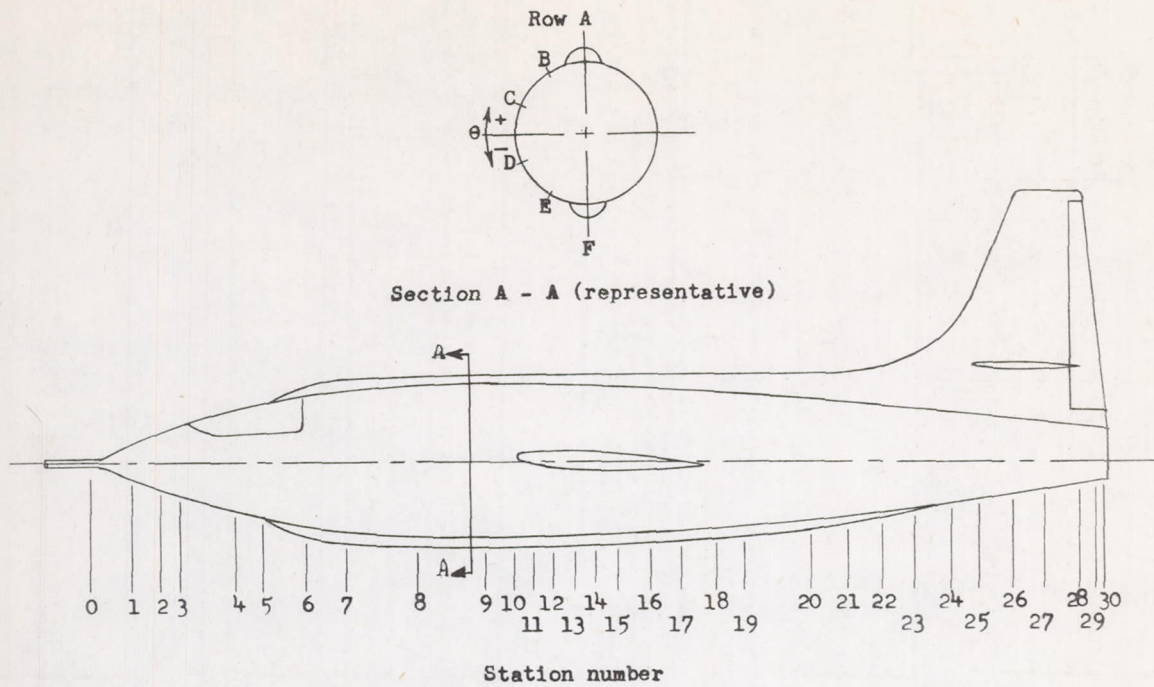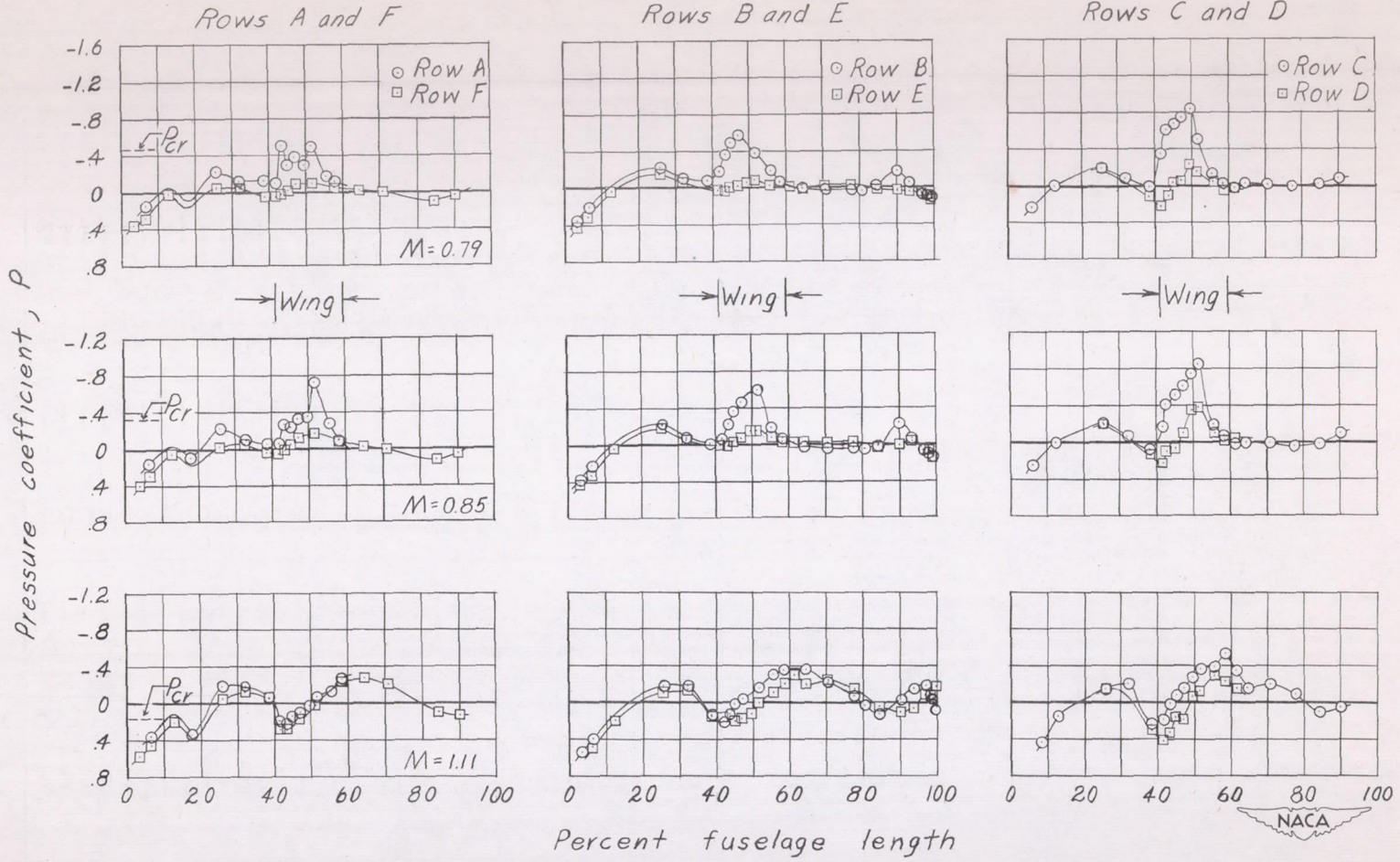Figure 1.— Overhead side view of Bell X-1 airplane.

Figure 2.- Three-view drawing of Bell X-1 airplane.

Row A

Section A - A (representative)

Station number

Figure 3.- Fuselage coordinates and locations of pressure measuring orifices.

| Station number	x/L	r/R	θ, deg					
			Row A	Row B	Row C	Row D	Row E	Row F
1	0.035	0.240	---	56.5	---	---	-52.2	-90
2	.065	.386	90	52.1	31.0	---	-53.4	-90
3	.086	.495	---	---	---	---	---	---
4	.127	.655	---	---	21.9	---	-50.5	-90
5	.175	.807	90	---	---	---	---	---
6	.210	.895	---	---	---	---	---	---
7	.259	.960	90	47.8	20.0	-19.8	-49.8	-90
8	.322	.996	90	47.9	20.1	---	-47.5	-90
9	.387	1.000	90	47.8	20.3	-19.7	-47.1	-90
10	.419	.999	90	49.2	20.8	-19.1	-48.2	-90
11	.435	.998	90	49.0	20.4	-19.1	-47.6	-90
12	.453	.996	90	48.7	20.1	-18.8	-47.1	-90
13	.471	.992	90	49.2	20.2	-18.9	-47.8	-90
14	.495	.981	90	49.6	20.4	-13.8	-46.5	---
15	.516	.974	90	49.6	20.3	-19.0	-48.7	-90
16	.556	.945	90	51.0	20.9	-19.3	-48.0	---
17	.582	.910	90	52.2	21.8	-19.8	-48.2	-90
18	.614	.873	---	---	22.4	-20.3	-48.3	---
19	.646	.833	---	52.4	23.8	-19.7	-48.2	-90
20	.709	.735	---	55.8	25.8	---	-48.3	-90
21	.742	.705	---	---	---	---	---	---
22	.775	.633	---	60.1	29.2	---	-49.9	-90
23	.807	.578	---	57.2	---	---	---	---
24	.841	.531	---	59.0	20.0	---	-47.8	-90
25	.871	.487	---	55.6	---	---	---	---
26	.901	.437	---	57.3	9.0	---	-49.5	-90
27	.932	.378	---	41.0	---	---	-44.0	---
28	.968	.327	---	58.0	---	---	-44.0	---
29	.984	.298	---	52.0	---	---	-45.0	---
30	.993	.280	---	47.0	---	---	-57.0	---

(a) $\alpha = 2^{\circ}$.

Figure 4.- Mach number effects on the pressure distributions along six
longitudinal rows on the fuselage of the Bell X-1 airplane. No data
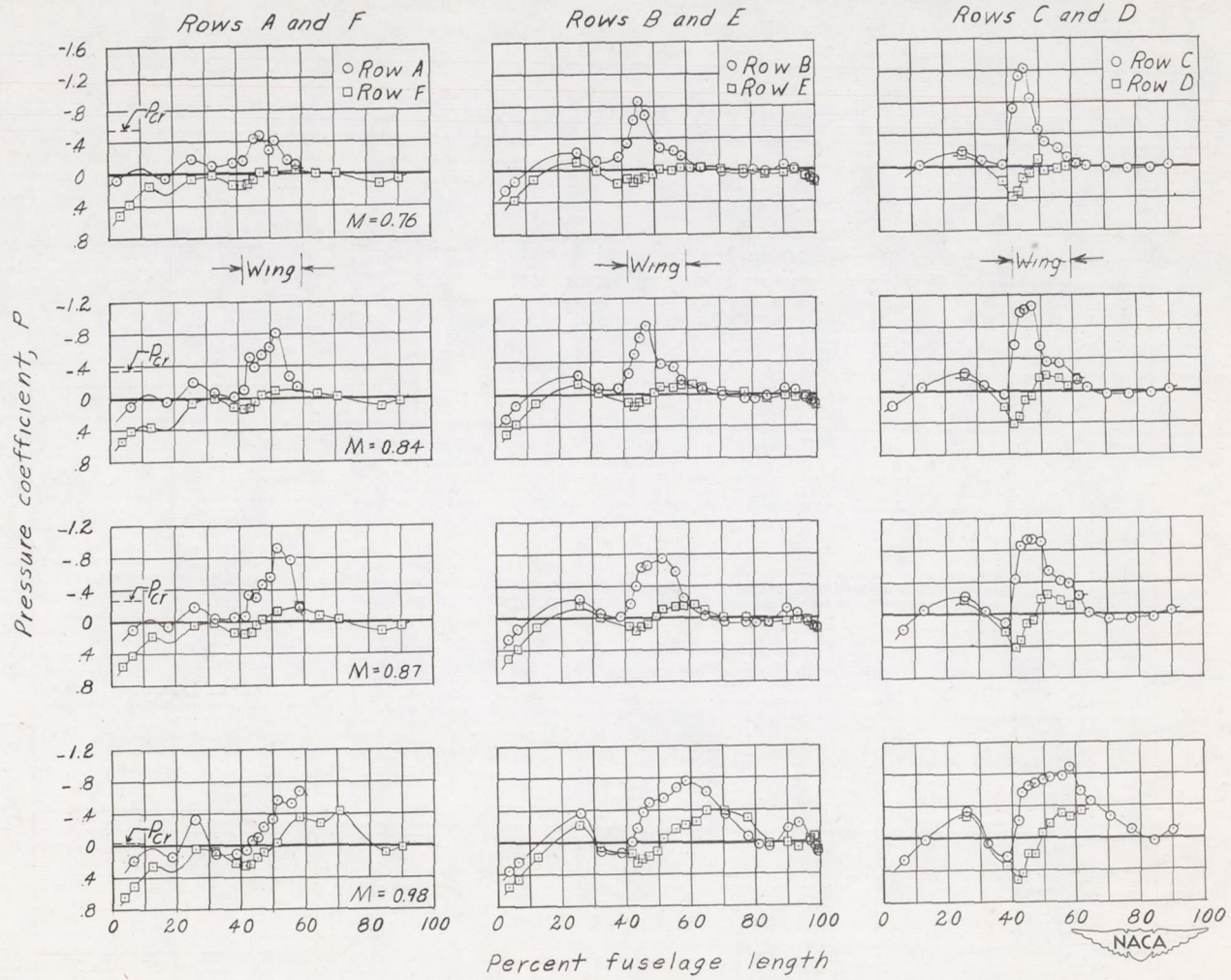available at $M = 0.88$ for $\alpha = 2^{\circ}$.
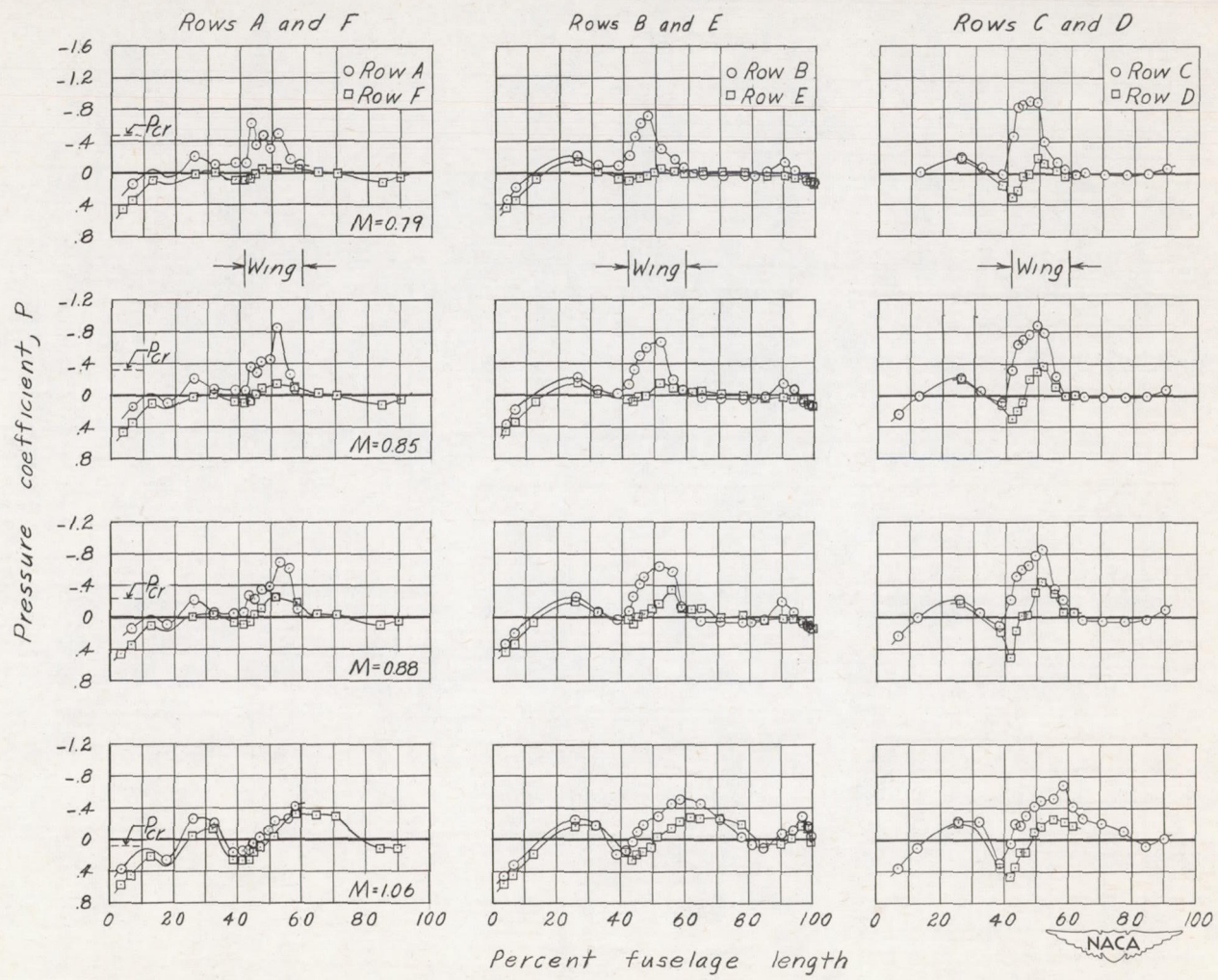
(b) α = 4°.

Figure 4.- Continued.
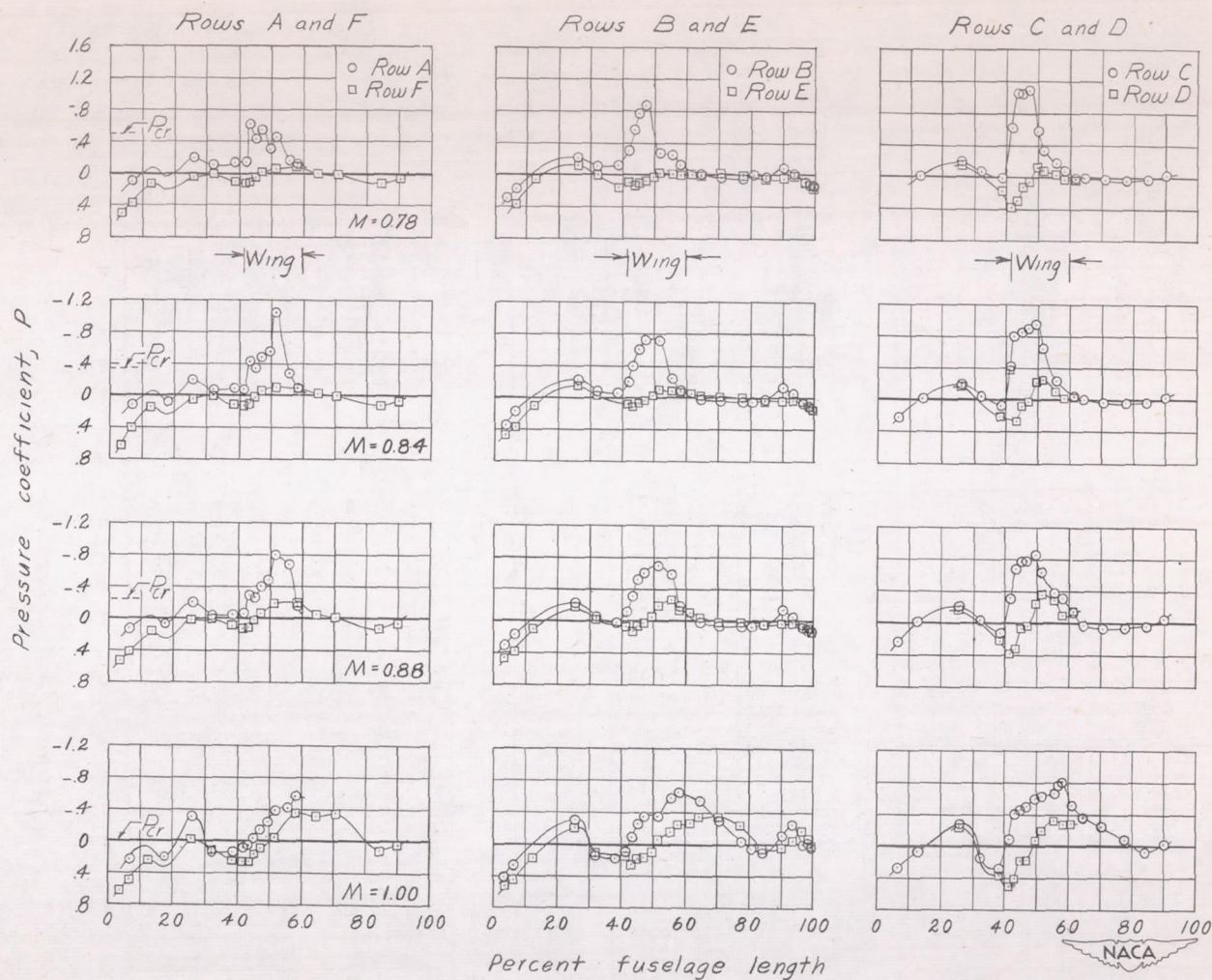
(c) α = 6°.

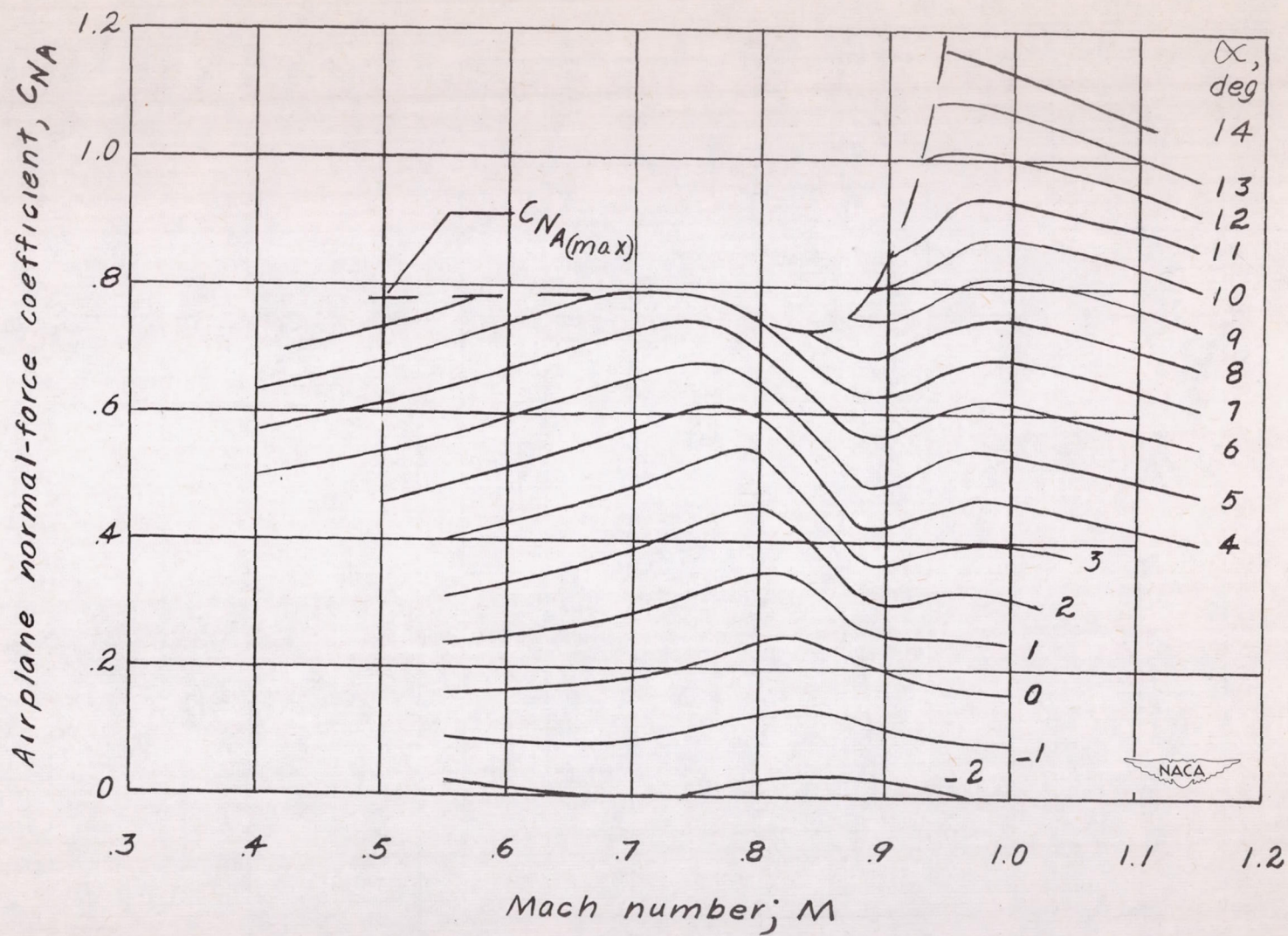Figure 4.- Continued.

(d) $\alpha = 8°$.

Figure 4.- Concluded.

Figure 5.- Approximate variation of airplane normal-force coefficient
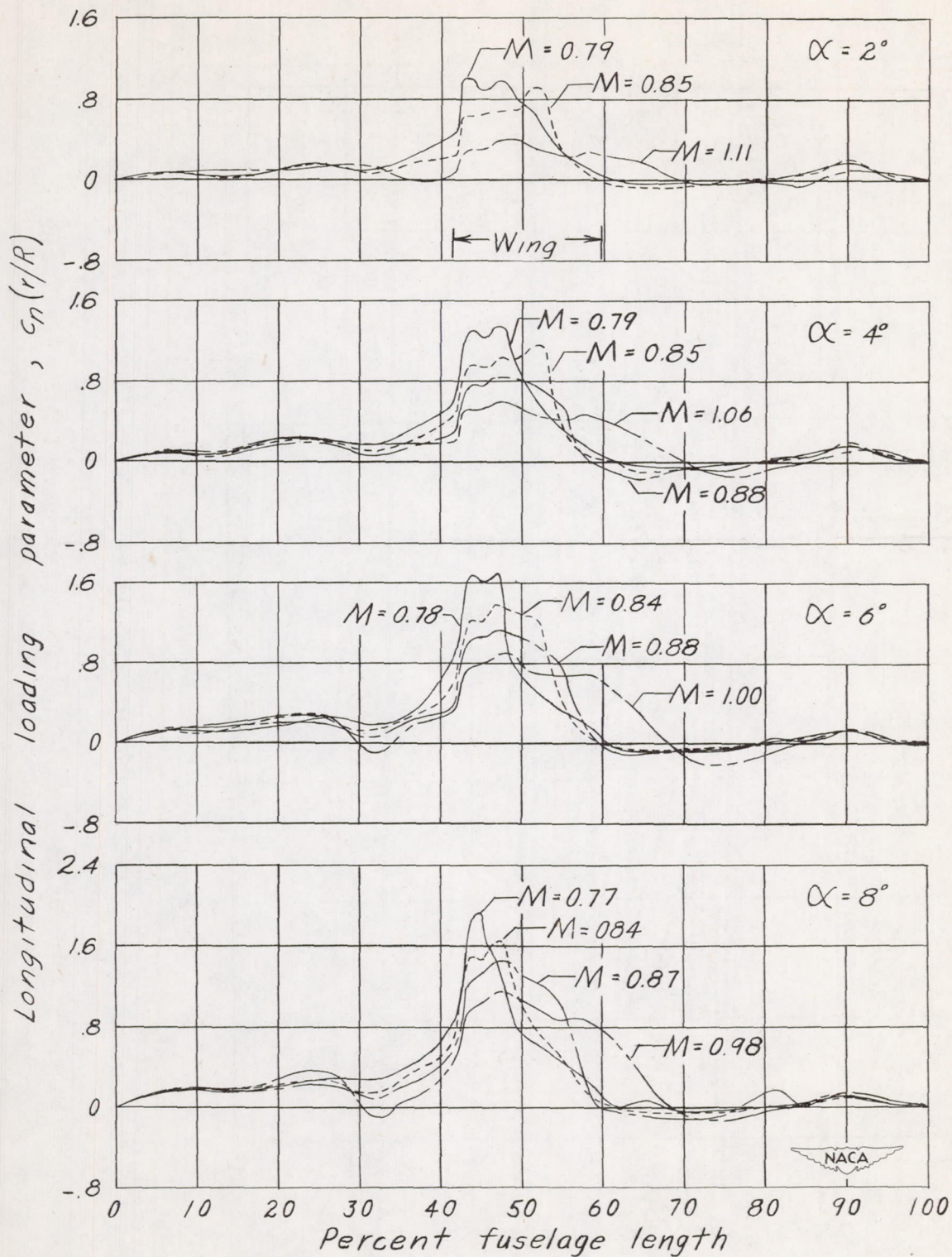with Mach number for various angles of attack.

Figure 6.- Mach number effects on the longitudinal fuselage load
distribution. α = 2° to 8°.

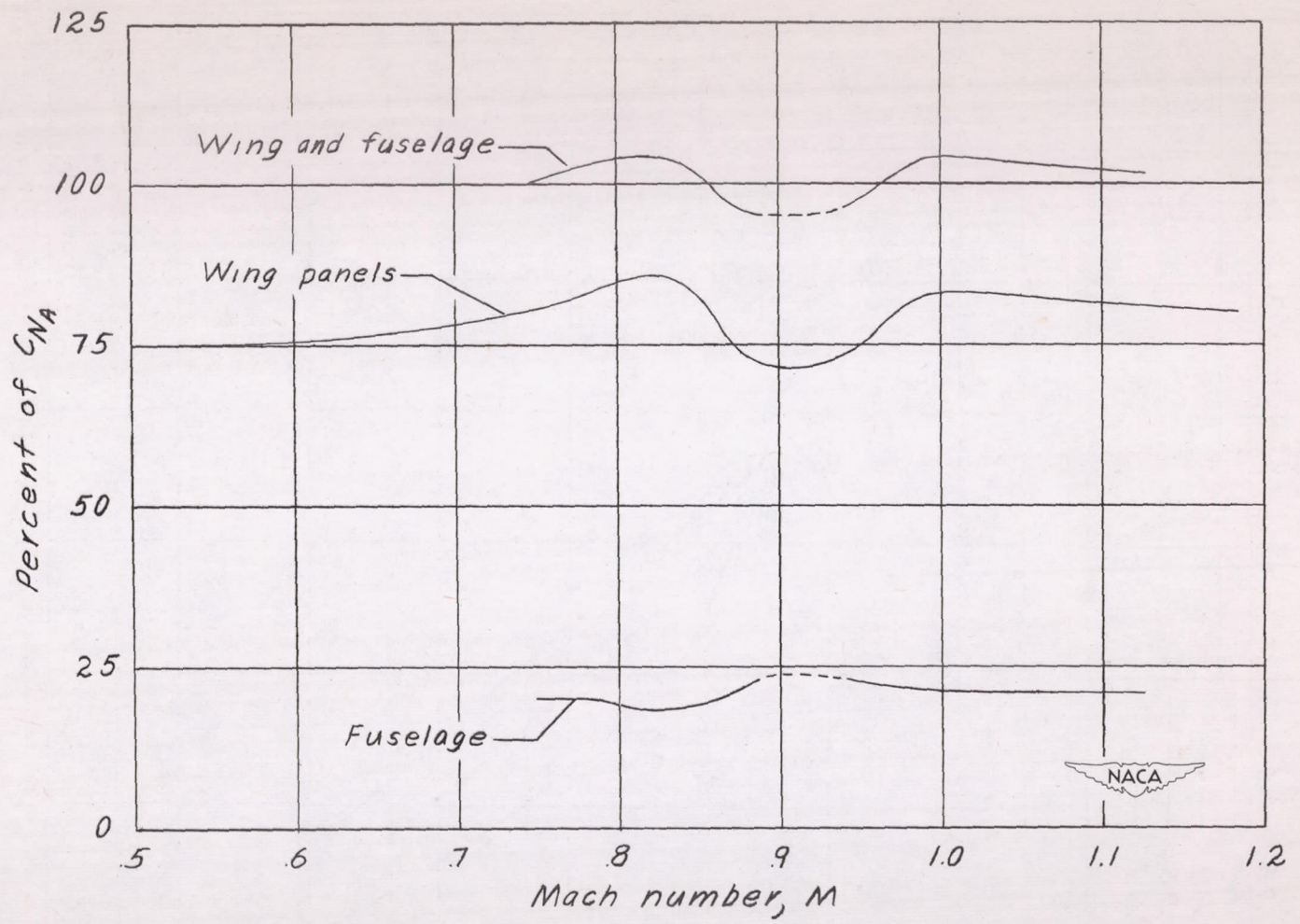Figure 7.- Approximate portion of the airplane normal-force coefficient carried by the wing panel, the fuselage, and the wing-fuselage combination. $C_{N_A} \approx 0.3$ to 0.7.
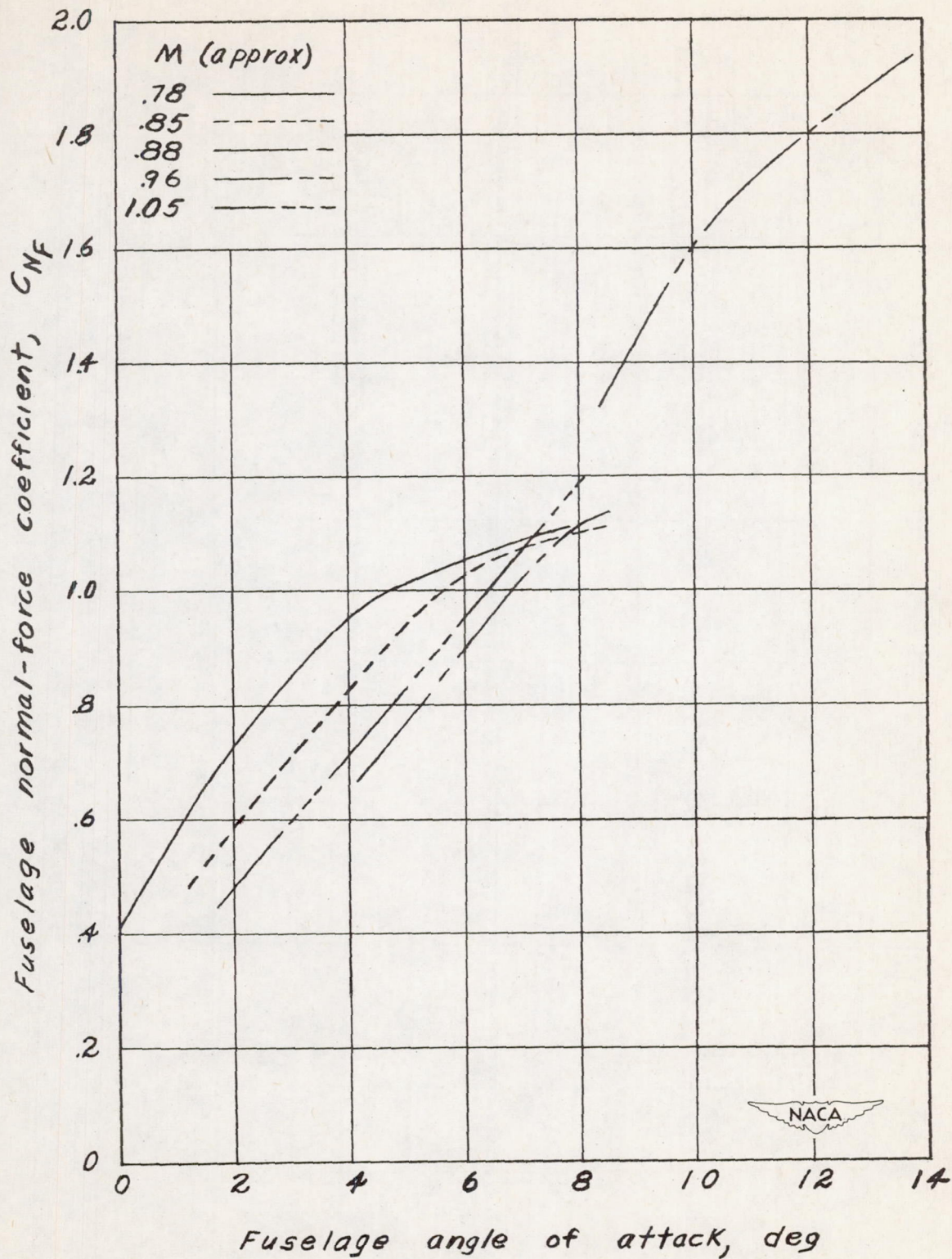
Figure 8.- Variation with angle of attack of fuselage normal-force coefficient.
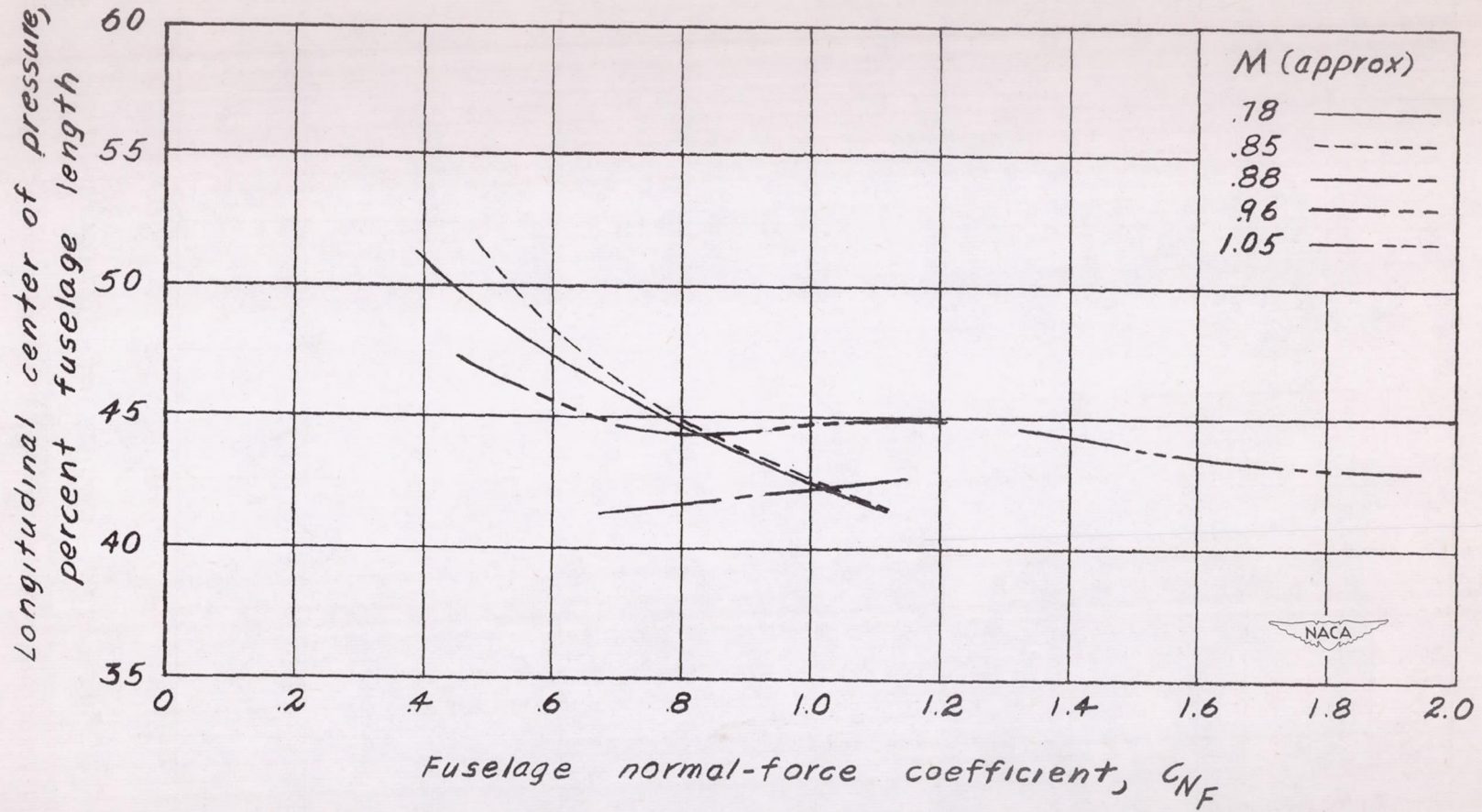
Figure 9.- Fuselage center-of-pressure variation with fuselage normal-force coefficient.